

The Effect of Annealing Temperature on Iron-Doped Tungsten Oxide Structure and Photosensitive Gas Sensor Applications

Sevda SARITAŞ^{1*}

¹ Atatürk University, Department of Electric Power Generation, Transmission and Distribution, İspir Hamza Polat Vocational College, Erzurum, Turkey.

Received: 05/04/2023, Revised: 15/04/2023, Accepted: 23/04/2023, Published: 31/08/2023

Abstract

In this study, changes in the crystal structure and gas sensor response will be investigated by doping iron to tungsten oxide structure and then annealing at 550°C. As a result of absorption - wavelength measurements, it was seen that the calculated band gap of the structure was between 3,08-3,15 eV. The direct optical band-gap energy (E_g) of thin films have been calculated by using the Tauc equation. It showed an increase of 0.7 eV as a result of the change in electronic configuration in the band gap. As a result of the heat treatment of the thin film, the absorption amount and the absorption wavelength have changed. Thus, an widening occurs in the optical band gap of the semiconductor. X-ray diffraction pattern of $WO_3:Fe$ films grown by sputter technique shows that the structure is amorphous, but after annealing at 550 °C in air, it is seen that a quality polycrystalline structure is formed, which supports this result in SEM images. All pronounced peaks of XRD patterns of $WO_3: Fe$ can be indexed to the cubic structure of tungsten oxide which present seven pronounced peaks (24°, 34°, 42°, 37.38°, 49°, 55°, 61°). Subsequently, the structural, optical and topographic properties of iron doped tungsten oxide ($WO_3:Fe$) structures grown by RF-DC co-sputter technique were investigated by scanning electron microscopy (SEM), atomic force microscopy (AFM), X-ray diffraction (XRD), and UV-VIS photospectroscopy techniques. The response of iron-doped tungsten oxide ($WO_3:Fe$) metal oxide structure grown by RF-DC co-sputtering to hydrogen gas was measured at flow values of 1000 ppm, at 300 °C temperature under white light and dark. All measurements were taken in the same cycle for 300 s, 180 s, and 120 s. and it has been seen that the examined thin films are suitable for gas sensor application under dark, are not suitable under white light.

Keywords: $WO_3:Fe$, Gas sensor, Photosensitive, Annealing

Tavlama Sıcaklığının Demir Katkılı Tungsten Oksit Yapısına ve Işığa Duyarlı Gaz Sensörü Uygulamalarına Etkisi

Öz

Bu çalışmada, demirin tungsten oksit yapısına katılanması ve ardından 550 °C'de tavlama ile kristal yapı ve gaz sensör tepkisindeki değişimler incelenecektir. Absorpsiyon-dalga boyu ölçümleri sonucunda yapının hesaplanan bant aralığının 3,08-3,15 eV arasında olduğu görüldü. İnce filmlerin doğrudan optik bant aralığı enerjisi (E_g), Tauc denklemi kullanılarak hesaplanmıştır. Bant aralığındaki elektronik konfigürasyondaki değişiklik sonucunda 0,7 eV'lik bir artış gösterdi. İnce filmin ısı işlemi sonucunda absorpsiyon miktarı ve absorpsiyon dalga boyu değişmiştir. Böylece yarı iletkenin optik bant aralığında bir genişleme meydana gelir. Püskürtme tekniği ile büyütülen $WO_3:Fe$ filmlerin X-ışını kırınım deseni yapının amorf olduğunu göstermektedir ancak havada 550 derecede tavlama sonrasında kaliteli bir polikristal yapı oluştuğu görülmektedir ki bu da SEM görüntülerinde bu sonucu desteklemektedir. $WO_3: Fe$ 'nin XRD modellerinin tüm belirgin tepe noktaları, yedi belirgin tepe noktası (24°, 34°, 42°, 37.38°, 49°, 55°, 61°) sunan tungsten oksitin kübik yapısına endekslenebilir. Daha sonra, RF-DC co-sputter tekniği ile büyütülen demir katkılı tungsten oksit ($WO_3:Fe$) yapılarının yapısal, optik ve topografik özellikleri taramalı elektron mikroskobu (SEM), atomik kuvvet mikroskobu (AFM), X-ışın kırınımı (XRD) ve UV-VIS foto spektroskopi teknikleri. RF-DC co-sputtering ile büyütülen demir katkılı tungsten oksit ($WO_3:Fe$) metal oksit yapısının hidrojen gazına tepkisi 1000 ppm akış değerlerinde, 300 °C sıcaklıkta beyaz ışık ve karanlıkta ölçülmüştür. Tüm ölçümler aynı döngüde 300 s, 180 s ve 120 s olarak alındı. İncelenen ince filmlerin karanlıkta gaz sensörü uygulamasına uygun olduğu, beyaz ışık altında ise uygun olmadığı görülmüştür.

Anahtar Kelimeler: $WO_3:Fe$, Gaz sensörü, Işığa duyarlılık, Tavlama

1. Introduction

Due to its electrochromic properties, tungsten oxide compound is a semiconductor material with an n-type carrier concentration, which is widely used in some application areas, especially due to its optical character. Metal oxide structures, whose optical properties are dominant, have recently attracted a lot of attention due to their applications in various technological fields and their properties. Its morphological structure, chemical composition, crystalline structure, and electrical, magnetic, and optical properties have made this material more useful in some technological applications and have been a source of inspiration for future studies [1,2]. Metal oxides, such as Fe_2O_3 [3] WO_3 [4,5] and NiO [6], which are widely used and widely used, have attracted great attention due to their morphological, optical and electronic properties that may be suitable for optoelectronic and electrochromic devices, and this interest will continue for a long time. it seems. In fact, the crystal structure, chemical properties and particle sizes of WO_3 thin films play a critical role in gas sensors [8,7] and in the photoanode for hydrogen production [9], while materials of tetragonal structure or amorphous oxides are used from electrochromic devices [10].

Especially harmful to the environment; Various techniques have been used to deposit metal oxide thin films for toxic, flammable and explosive gas detection applications [11-16]. Thin film deposition processes always have advantages and disadvantages such as cost, vacuum requirement, high temperature, quality substrate. The toxic, flammable and explosive gas detection properties of metal oxides are determined by their crystal properties and crystal size, but can also be improved by adding various proportions of impurities, reducing particle size, and changing the surface morphology and particle size of the films. The gas sensing ability of thin films is limited to the surface layer and cannot penetrate deeper regions, whereas thicker films are generally porous and thus can interact with any gas layer. The gas sensing properties of thin films can be significantly improved in a variety of ways, including speed, response rate, and turnaround time [17].

In some experimental studies, it has been observed that film thickness, grain size, chemical structure and crystal structure can have a significant effect on improving sensor selectivity and sensitivity. Gas detection sensitivity also depends on the film surface, as sensors are greatly affected by moisture on the surface and the presence of oxidizing or reducing gases. The quality of the sensors can be improved by adding various proportions of impurities to the surface of the films and adding a certain amount of defective active species. The incorporation of different additive metals into oxide films has been shown to increase the sensitivity to certain gases [18]. In this study, changes in the crystal structure and gas sensor response will be investigated by doping iron to the tungsten oxide structure and then annealing at 550 °C.

2. Material and Methods

The sputtering technique is the growth of ions, atoms, and molecules broken from the metal target on the heated substrate cleaned by chemical processes as a thin film with the help of inert gas. In order to break the material to be grown from the metal target, argon is turned into an inert gas carrier plasma with the help of an RF or DC power source and the plasma performs

the detachment process by beating the surface of the target metal. The tungsten sputtering target has 2 inches (dia) x 0.125 inches (thickness) and the iron metal target has 2 inches (dia) x 0.125 inches (thickness). An iron target was placed in the DC power gun and a tungsten target was placed in the RF gun source.

In this experimental study, an iron target was attached to the DC power supply and a tungsten target was attached to the RF power supply part. While the DC power supply is 100 watts, the RF power supply is set to 50 watts. The glass substrates placed for the vacuum chamber up to 4×10^{-6} torr pressure (base pressure) were heated up to 450 degrees. Then 100 cubic centimeters per minute (sccm) of inert argon gas was sent in and plasma was formed. Then, 42 sccm of argon and 3 sccm of oxygen gas were given to grown pressure of 8.5×10^{-3} torr and growth was made for 45 minutes. Subsequently, the structural, optical and topographic properties of iron doped tungsten oxide ($\text{WO}_3:\text{Fe}$) structures grown by RF-DC co-sputter technique were investigated by SEM, AFM, XRD, and UV-VIS photospectroscopy techniques.

XPS measurements were carefully made with the FlexMod Specs XPS system, which can measure very precisely. An Al anode operating at 15 kV, 400 W was used as an X-ray source, which is one of the important technical information of the system where the measurements were taken (Excitation energy: 1486.71 eV, Binding energy: 1387 eV, Transition energy: 75 eV, Bias voltage: 65 V, Detector voltage: 1580V, Scan mode: Fixed Analyzer Transmission). The no-load corrected C1s signal generally ranged from 284.5 eV to 285 eV, based on measurements made with a large number of important conductive samples and a routinely continuously calibrated instrument. The sample was spray etched with a 0.5 keV Ar^+ ion beam incident at an angle of 70° from the surface normal.

$\text{WO}_3:\text{Fe}$ structure, human-made detection system that can detect various flammable, explosive and toxic gases, and H_2 sensor detection tests have been carried out. The gas sensor test system consists of a device with a characterization probe capable of taking IV (ampere-volt) measurement, a low and high temperature control unit and a highly sensitive gas flow meter. Two mass flow controller units are available to achieve dry air and different (dry air + H_2) H_2 ppm levels. All electrical measurement of the sensor under different hydrogen levels was measured with Keithley 487 pico ammeter/voltage source and all devices were controlled by software that can evaluate very precise measurements. H_2 gas with various standard sccm was mixed with 500 sccm of dry air to achieve desired H_2 parts per million (ppm) levels of 1000 ppm at 300°C set prior to gas detection measurements. In order to take measurements correctly, each sensor measurement cycle was started in a dry air environment of certain purity, then 1000 ppm H_2 gas was sent to the test room where the measurement was taken, accompanied by dry air, and a 2 V constant voltage electricity was supplied with a suitable voltage source in the different gas environment where this measurement is desired. current was measured against time. By giving 99.99 percent pure oxygen gas to the system, it was aimed to clean all gaseous pollution that could adversely affect the measurements other than oxygen for two hours at 300°C . By giving high purity and high flow oxygen (500 sccm) gas to the system, the substrate was heated up to 300°C and all gas contamination, surface impurities and moisture inside were tried to be cleaned for two hours. To obtain different H_2 and dry air ppm level in systems gas, two

Alicat Mass Flow Controllers, which are controlling in different flow levels 0–0.5 sccm and 0–500 sccm, were used and total flow fixed to 500 sccm by this system .

The response of iron doped tungsten oxide ($\text{WO}_3:\text{Fe}$) structure grown by RF-DC co-sputtering to hydrogen gas was measured at flow values of 1000 ppm, at 300 °C temperature under white light and dark. All measurements were taken in the same cycle for 300 s, 180 s, and 120 s.

3. Results and Discussion

Firstly, the as-grown $\text{WO}_3:\text{Fe}$ structure was annealed in a two-stage furnace at 550 °C. With the annealing process showed a serious change in the crystal structure of the thin film, and it showed a serious change in its optical properties. The thickness of the thin films was measured as 400 nm with the "Kla Tencor Stylus Profiler P7" device.

As a result of optical measurements, it was seen that the band gap of the structure was between 3,08-3,15 eV. The direct optical band-gap energy (E_g) of thin films have been calculated by using the Tauc equation. It showed an increase of 0.7 eV as a result of the change in electronic configuration in the band gap. As seen in Figure 1a, as a result of the heat treatment of the thin film, the absorption amount and the absorption wavelength have changed. Thus, an widening occurs in the optical band gap of the semiconductor (Fig.1b).

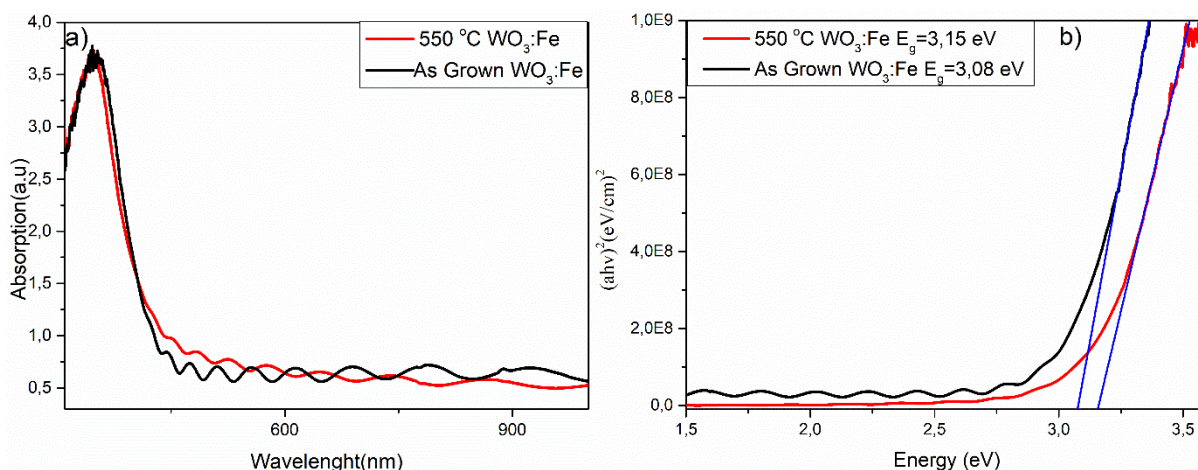


Figure 1. a) Absorption graph of as grown $\text{WO}_3:\text{Fe}$ and 550°C annealed $\text{WO}_3:\text{Fe}$ b) Band gap graph of as grown $\text{WO}_3:\text{Fe}$ and 550°C annealed $\text{WO}_3:\text{Fe}$

All pronounced peaks of XRD patterns of $\text{WO}_3:\text{Fe}$ showed in Figure 2(a) can be indexed to the cubic structure of tungsten oxide which presents seven pronounced peaks (24° , 34° , 42° , 37.38° , 49° , 55° , 61°) (Reference code: 00-041-0905). The peaks seen in the XRD graph were found to be consistent with the literature [17]. X-ray diffraction pattern of $\text{WO}_3:\text{Fe}$ films grown by sputter technique shows that the structure is amorphous, but after annealing at 550 degrees in air, it is seen that a quality polycrystalline structure is formed, which supports this result in SEM images. The XRD patterns of the film grown on glass substrate have been shown in figure. As seen in figure $\text{WO}_3:\text{Fe}$ thin film grown on glass substrate has polycrystalline orientation along different planes and phases.

The crystallite size was calculated using Debye-Scherrer formula, $D(\text{nm})=0.94 \lambda / \beta \cos \theta$ where λ is the wavelength ($\lambda = 1.5405 \text{ \AA}$), β is the full width at half maximum (FWHM) of the

considerate peak and θ is the corresponding Bragg's angle. As grown $\text{WO}_3:\text{Fe}$, 550°C annealed $\text{WO}_3:\text{Fe}$ crystal grain sizes of film are $D=50\text{ nm}$ and $D=4\text{ nm}$, respectively.

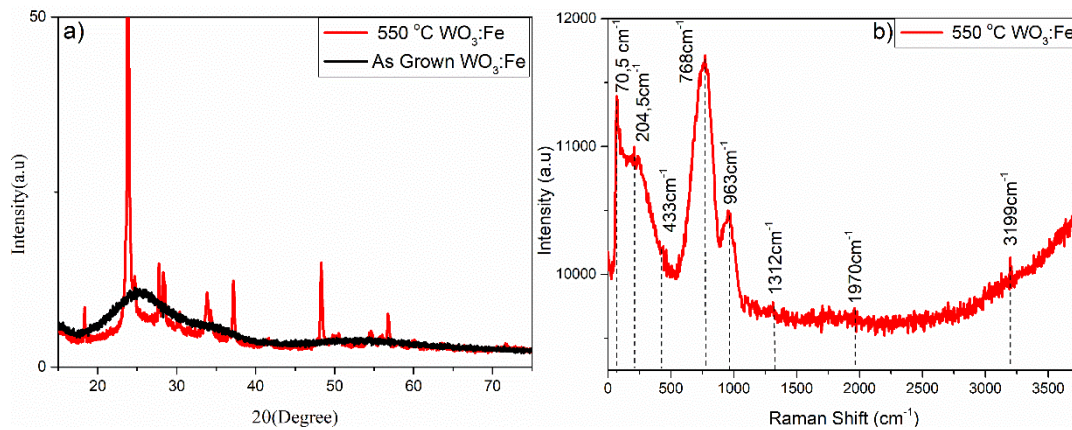


Figure 2. a) XRD graph of as grown $\text{WO}_3:\text{Fe}$ and 550°C annealed $\text{WO}_3:\text{Fe}$ b) Raman shift graph of 550°C annealed $\text{WO}_3:\text{Fe}$

As shown in Fig. 2b, two typical broad Raman bands in the range of $200\text{--}500\text{ cm}^{-1}$ and $550\text{--}1050\text{ cm}^{-1}$ were observed. The first band ($200\text{--}500\text{ cm}^{-1}$) is associated with O -W - O bending modes, whereas the second band is related to stretching modes.

Raman spectroscopy was employed to characterize the chemical properties and crystalline nature of the 550°C annealed $\text{WO}_3:\text{Fe}$ thin films. Raman peaks of the annealed sample were seen with peak positions at about 70 cm^{-1} , 204 cm^{-1} , 433 cm^{-1} (O -W - O bending modes Ag_1), 768 cm^{-1} and 963 cm^{-1} , (stretching modes E_g) respectively.

Raman peaks of the film are at positions of about 963 cm^{-1} and 768 cm^{-1} (Fig. 2b) and are usually assigned in the literature to the stretching frequency modes of bridging oxygen W-O and O-W-O, respectively.

In the SEM image (Fig 3a-b), it is seen that the structure is distributed very homogeneously on the substrate. The cubic structure is clearly visible. Energy dispersive X-ray spectroscopy is an analytical technique that provides chemical characterization/element analysis of materials. The data obtained with this technique are given. In the EDX results, the presence of Fe, W and O at certain ratios in the thin film was detected 4%, 56%, 40%, respectively.

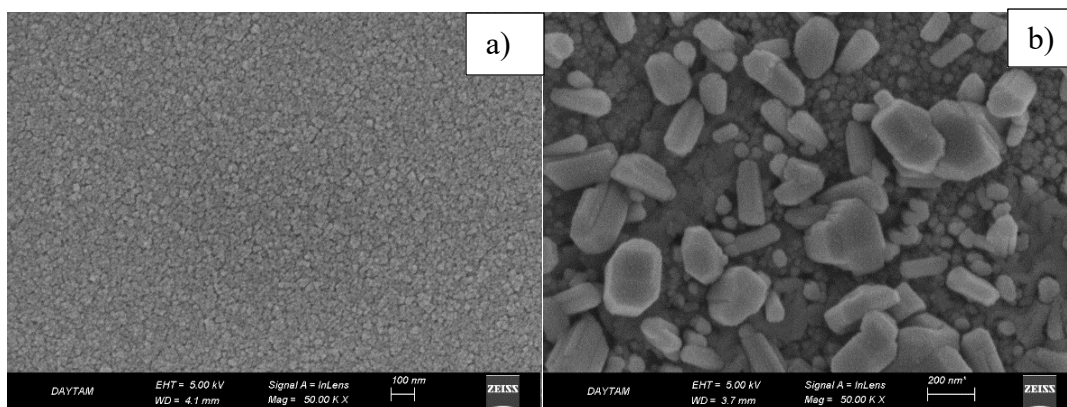


Figure 3. SEM images of the a) as grown $\text{WO}_3:\text{Fe}$ b) 550°C annealed $\text{WO}_3:\text{Fe}$

The surface morphology of the as grown $\text{WO}_3:\text{Fe}$, 550°C annealed $\text{WO}_3:\text{Fe}$ (Fig.4a-b) thin films was analysed using the non-contact mode of AFM. Figure 4 shows 2D and 3D AFM images of the as grown $\text{WO}_3:\text{Fe}$, 550°C annealed $\text{WO}_3:\text{Fe}$ films grown on glass substrates at 8.5 mTorr grown pressure. Roughness values of film are $R_a= 1.5$ nm, $S_a=4.3$ nm and $R_a= 21$ nm, $S_a=29$, respectively.

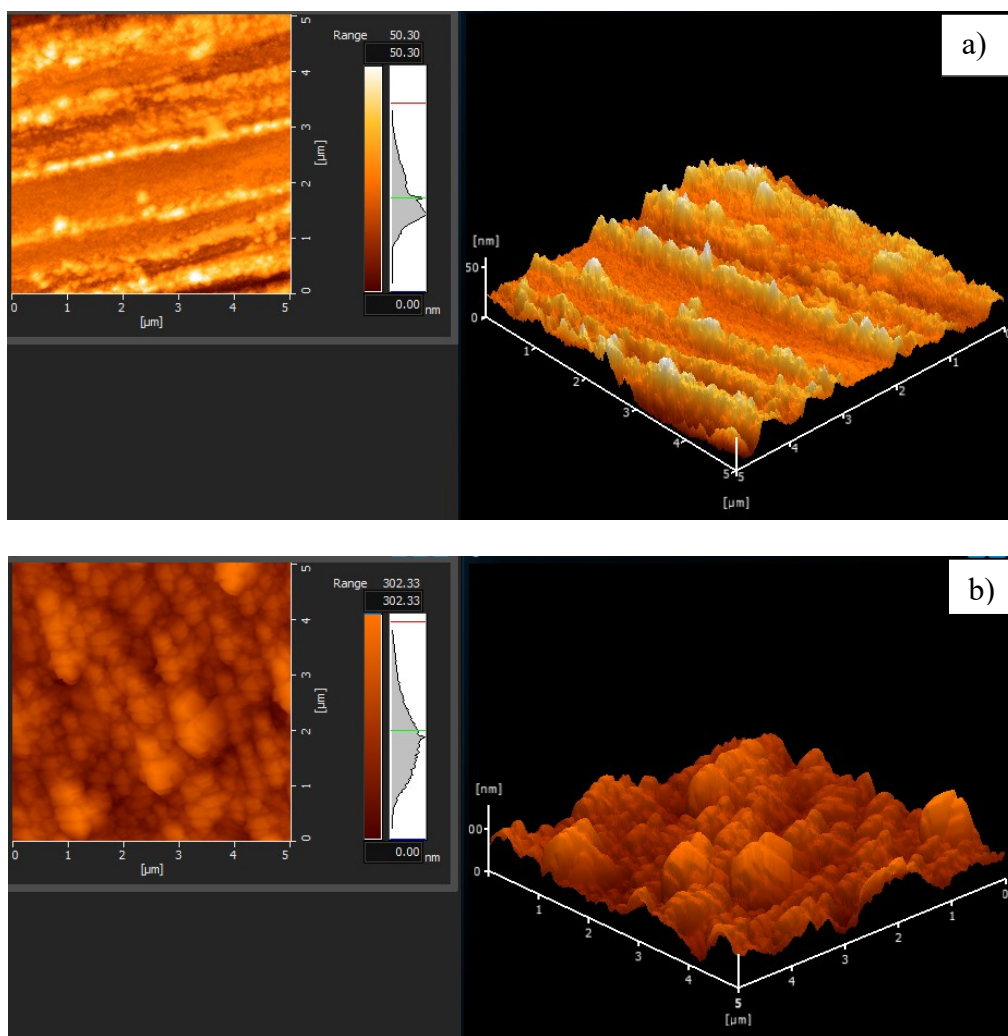


Figure 4. 2D and 3D AFM images of the **a)** as grown $\text{WO}_3:\text{Fe}$ **b)** 550°C annealed $\text{WO}_3:\text{Fe}$

The XPS binding energy of ferrous metal is 706.7 eV, and the XPS binding energy of tungsten metal is ($4f_{7/2}$) 31.30 eV. In the literature, this value is 709.6 for FeO and 710.8 eV for Fe_2O_3 . Likewise, this value for WO_3 is 33.95 eV. In our study (Fig. 5a, 5b, 5c,5d), while the XPS binding energy for iron is 712.14 eV, this value is 35.04 eV for tungsten. So, it can be concluded that there are iron-oxygen bonds, tungsten-oxygen bonds, and also iron- tungsten -oxygen bonds.

As a result of XPS measurements, it is seen in many studies that two main peaks are detected at the W4f level and that the $\text{W}6^+$ state is referred to at 35.25 and 37.40 eV of the binding energies of $4f_{7/2}$ and $4f_{5/2}$. In addition, two low-intensity peaks attributed to the presence of the W^{5+} state at binding energies of 33.95 and 36.10 eV, and often the presence of oxygen vacancies of these two low peaks have been confirmed in many studies. Similarly, W4f core level XPS

spectra of Fe-doped WO₃ revealed two pairs for each of the W⁶⁺ and W⁵⁺ states. However, as a result of careful observations, it is seen in this study, as in many studies, that the peak density of the W⁵⁺ state shows a significant increase after the addition of Fe.

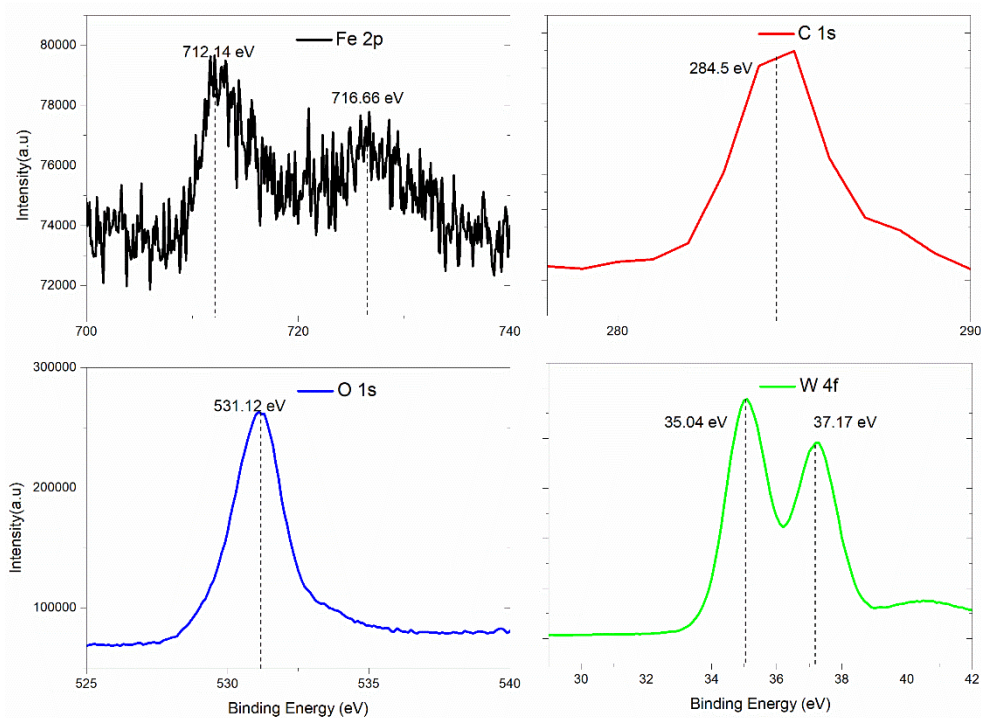


Figure 5. a) XPS spectra for W 4f b) Fe 2p c) O 1s d) C 1s of WO₃:Fe thin film

For gas sensor measurements, comb-shaped interdigitate electrodes (IDT), which can give more sensitive and accurate results, were produced with Ag metal spraying, which is the most suitable metal. In this study, measurements were also taken with different metals, but the results could not provide the desired quality data. The IDT contact distance between the electrodes is 500 μm and the total surface of the measured area is 1.2 cm x 1.2 cm. The sensor metal Ag was sputtered onto the sample using the sputter technique. H₂ gas with various standard sccms was mixed with 500 sccm of dry air to achieve desired H₂ parts per million (ppm) levels of 1000 ppm set at 300 °C set prior to gas detection measurements. Appropriate action was taken to clean the inside of the system before starting the measurement. A full cycle of each sensor measurement was started in a dry air environment in order to obtain accurate results, then 1000 ppm dry air + H₂ gas was sent to the gas sensor test room, and the electric current produced by the voltage source and charge carriers was measured in this different gas environment at a constant voltage of 2 V.

When the oxygen gas on the film surface is held by hydrogen (dry air +H₂), the free electrons of the oxygen provide an excess negative charge at the band edge and combine with the film, which is a p-type semiconductor material. vacancies in the valence band with this excess electron. This results in a smaller current (hole+electron=recombination). This phenomenon reduces the conductivity of the material (Fig. 6).

In the study, the working principle of gas sensors is based on the conductivity changes produced when the sensing material is exposed to target gases. The conductivity change is based on gas molecule adsorption and electron exchange between particles in the reaction state

on the semiconductor surface. The gas sensor response was made according to the equation $[\%R=(I_0-I) \times 100]$. Here, R is sensors response. I_0 is first current, and I is finally current.

The measurements were performed at 300 °C to 1000 ppm H_2 gas. $WO_3:Fe$ thin films show 7.1% response (light) and 18.6% response to 1000 ppm H_2 gas at 300 °C.

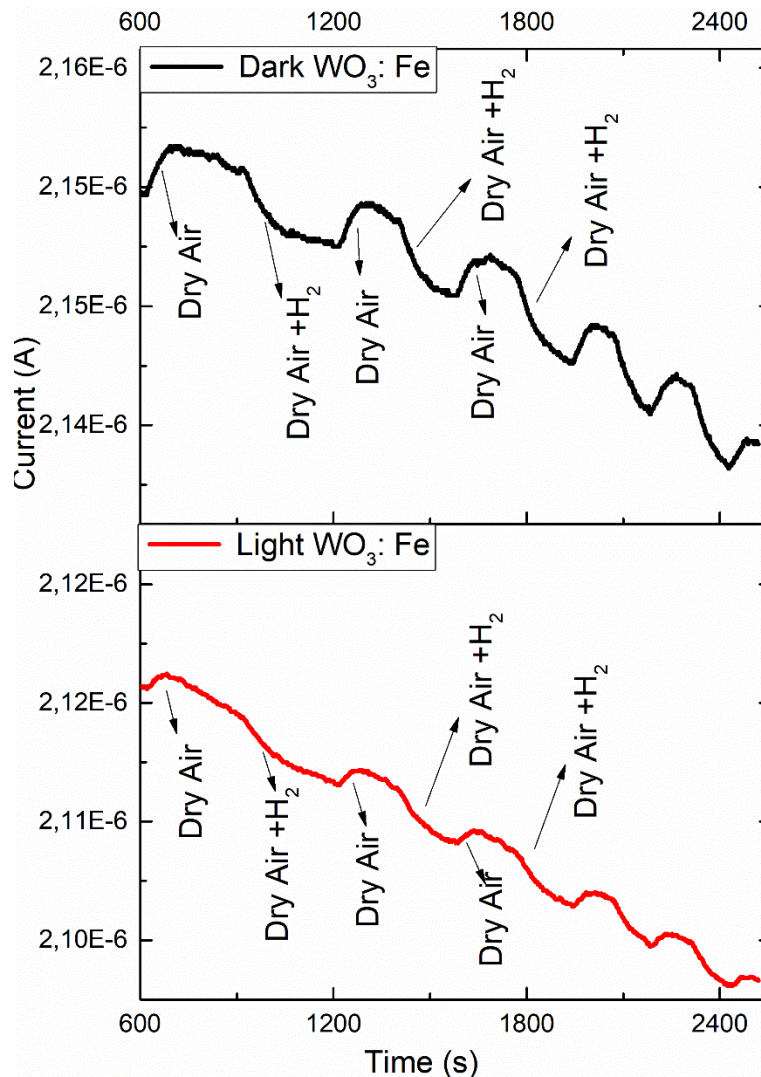


Figure 6. Gas sensors response of $WO_3:Fe$ for 1000ppm at 300°C under light and dark

4. Conclusion

X-ray diffraction pattern of $WO_3:Fe$ films grown by sputter technique shows that the structure is amorphous, but after annealing at 550 degrees in air, it is seen that a quality polycrystalline structure is formed, which supports this result in SEM images. All pronounced peaks of XRD patterns of $WO_3:Fe$ showed, can be indexed to the cubic structure of tungsten oxide which presents seven pronounced peaks. As grown $WO_3:Fe$, 550°C annealed $WO_3:Fe$ crystal grain sizes of film are $D=50\text{ nm}$ and $D=4\text{ nm}$, respectively. As a result of optical measurements, it was seen that the band gap of the structure was between 3,08-3,15 eV. As grown $WO_3:Fe$, 550°C annealed $WO_3:Fe$ roughness values of film are $Ra=1.5\text{ nm}$, $Sa=4.3\text{ nm}$ and $Ra=21\text{ nm}$, $Sa=29$, respectively.

XPS binding energy for iron is 712.14 eV, this value is 35.04 eV for tungsten. So, it can be concluded that there are iron-oxygen bonds, tungsten-oxygen bonds, and also iron-tungsten-oxygen bonds. The response of iron doped tungsten oxide ($\text{WO}_3:\text{Fe}$) structure grown by RF-DC co-sputtering to hydrogen gas was measured at flow values of 1000 ppm, at 300 °C temperature under white light and dark. All measurements were taken in the same cycle for 300 s, 180 s, and 120 s. And it has been seen that the examined thin films are suitable for gas sensor application in dark but are not suitable under white light. The measurements were performed at 300 °C to 1000 ppm H_2 gas. $\text{WO}_3:\text{Fe}$ thin films show 7.1% response (light) and 18.6% response to 1000 ppm H_2 gas at 300 °C.

Ethics in Publishing

There are no ethical issues regarding the publication of this study.

Acknowledgment

The present work was supported by Ataturk University.

References

- [1] W. Kim, J.K. Kim, Y. Lim, I. Park, Y.S. Choi, J.H. Park, Tungsten oxide/PEDOT:PSS hybrid cascade hole extraction layer for polymer solar cells with enhanced long-term stability and power conversion efficiency, *Sol. Energy Mater. Sol. Cells* 122 (2014) 24–30.
- [2] M. Vasilopoulou, D. Davazoglou, Hot-wire vapor deposited tungsten and molybdenum oxide films used for carrier injection/transport in organic optoelectronic devices, *Mater. Sci. Semicond.* 16 (2013) 1196–1216.
- [3] Saritas, S., Kundakci, M., Coban, O., Tuzemen, S., & Yildirim, M. (2018). Ni: Fe_2O_3 , Mg: Fe_2O_3 and Fe_2O_3 thin films gas sensor application. *Physica B: Condensed Matter*, 541, 14-18.
- [4] N. Li, T. Stubhan, N.A. Luechinger, S.C. Halim, G.J. Matt, T. Ameri, C.J. Brabec, Inverted structure organic photovoltaic devices employing a low temperature solution processed WO_3 anode buffer layer, *Org. Electron.* 13 (2012) 2479–2484.
- [5] T. Ripolles-Sanchis, A. Guerrero, E. Azaceta, R. Tena-Zaera, G. Garcia-Belmonte, Electrodeposited NiO anode interlayers: enhancement of the charge carrier selectivity in organic solar cells, *Sol. Energy Mater. Sol. Cells* 117 (2013) 564–568.
- [6] Turgut, E., Çoban, Ö., Saritaş, S., Tüzemen, S., Yıldırım, M., & Gür, E. (2018). Oxygen partial pressure effects on the RF sputtered p-type NiO hydrogen gas sensors. *Applied Surface Science*, 435, 880-885.
- [7] D.B. Hernandez-Uresti, D. Sánchez-Martínez, A. Martínez-de la Cruz, S. Sepúlveda-Guzmán, L.M. Torres-Martínez, Characterization and photocatalytic properties of hexagonal and monoclinic WO_3 prepared via microwave-assisted hydrothermal synthesis, *Ceram. Int.* 40 (2013) 9–22.

- [8] N. Datta, N. Ramgir, M. Kaur, M. Roy, R. Bhatt, S. Kailasaganapathi, A.K. Debnath, D.K. Aswal, S.K. Gupta, Vacuum deposited WO₃ thin films based sub-ppm H₂S sensor, *Mater. Chem. Phys.* 134 (2012) 851–857.
- [9] N. Naseri, H. Kim, W. Choi, A.Z. Moshfegh, Implementation of Ag nanoparticle incorporated WO₃ thin film photoanode for hydrogen production, *Int. J. Hydrog. Energy* 38 (2013) 2117–2125.
- [10] K. Sauvet, A. Rougier, L. Sauques, Electrochromic WO₃ thin films active in the IR region, *Sol. Energy Mater. Sol. Cells* 92 (2008) 209–215.
- [11] Cantalini, C., Sun, H. T., Faccio, M., Pelino, M., Santucci, S., Lozzi, L., & Passacantando, M. (1996). NO₂ sensitivity of WO₃ thin film obtained by high vacuum thermal evaporation. *Sensors and Actuators B: Chemical*, 31(1-2), 81-87.
- [12] Sivakumar, R., Jayachandran, M., & Sanjeeviraja, C. (2004). Studies on the effect of substrate temperature on (VI–VI) textured tungsten oxide (WO₃) thin films on glass, SnO₂: F substrates by PVD: EBE technique for electrochromic devices. *Materials Chemistry and Physics*, 87(2-3), 439-445.
- [13] Siciliano, T., Tepore, A., Micocci, G., Serra, A., Manno, D., & Filippo, E. (2008). WO₃ gas sensors prepared by thermal oxidation of tungsten. *Sensors and Actuators B: Chemical*, 133(1), 321-326.
- [14] Choi, Y. G., Sakai, G., Shimanoe, K., Miura, N., & Yamazoe, N. (2003). Wet process-prepared thick films of WO₃ for NO₂ sensing. *Sensors and Actuators B: Chemical*, 95(1-3), 258-265.
- [15] Ederth, J., Hoel, A., Niklasson, G. A., & Granqvist, C. G. (2004). Small polaron formation in porous WO_{3-x} nanoparticle films. *Journal of applied physics*, 96(10), 5722-5726.
- [16] Song, S. K., Cho, J. S., Choi, W. K., Jung, H. J., Choi, D., Lee, J. Y., ... & Koh, S. K. (1998). Structure and gas-sensing characteristics of undoped tin oxide thin films fabricated by ion-assisted deposition. *Sensors and Actuators B: Chemical*, 46(1), 42-49.
- [17] Stankova, M., Vilanova, X., Calderer, J., Llobet, E., Brezmes, J., Gracia, I., ... & Correig, X. (2006). Sensitivity and selectivity improvement of rf sputtered WO₃ microhotplate gas sensors. *Sensors and Actuators B: Chemical*, 113(1), 241-248.
- [18] Rothschild, A., Edelman, F., Komem, Y., & Cosandey, F. (2000). Sensing behavior of TiO₂ thin films exposed to air at low temperatures. *Sensors and Actuators B: Chemical*, 67(3), 282-289.